The Astrophysical Journal Letters, 856:L25 (4pp), 2018 April 1 https://doi.org/10.3847/2041-8213/aab61e

Chandra X-Rays from the Redshift 7.54 Quasar ULAS J1342+0928

Eduardo Bañados[1,7], Thomas Connor[1], Daniel Stern[2], John Mulchaey[1], Xiaohui Fan[3], Roberto Decarli[4], Emanuele P. Farina[5], Chiara Mazzucchelli[6], Bram P. Venemans[6], Fabian Walter[6], Feige Wang[5], and Jinyi Yang[3]
[1] The Observatories of the Carnegie Institution for Science, 813 Santa Barbara Street, Pasadena, CA 91101, USA; ebanados@carnegiescience.edu
[2] Jet Propulsion Laboratory, California Institute of Technology, 4800 Oak Grove Drive, Pasadena, CA 91109, USA
[3] Steward Observatory, The University of Arizona, 933 North Cherry Avenue, Tucson, AZ 85721-0065, USA
[4] INAF–Osservatorio di Astrofisica e Scienza dello Spazio, via Gobetti 93/3, I-40129 Bologna, Italy
[5] Department of Physics, Broida Hall, University of California, Santa Barbara, CA 93106-9530, USA
[6] Max Planck Institut für Astronomie, Königstuhl 17, D-69117 Heidelberg, Germany
Received 2018 February 8; revised 2018 February 27; accepted 2018 March 6; published 2018 March 27

Abstract

We present a 45 ks *Chandra* observation of the quasar ULAS J1342+0928 at $z = 7.54$. We detect $14.0^{+4.8}_{-3.7}$ counts from the quasar in the observed-frame energy range 0.5–7.0 keV (6σ detection), representing the most distant non-transient astronomical source identified in X-rays to date. The present data are sufficient only to infer rough constraints on the spectral parameters. We find an X-ray hardness ratio of $\mathcal{HR} = -0.51^{+0.26}_{-0.28}$ between the 0.5–2.0 keV and 2.0–7.0 keV ranges and derive a power-law photon index of $\Gamma = 1.95^{+0.55}_{-0.53}$. Assuming a typical value for high-redshift quasars of $\Gamma = 1.9$, ULAS J1342+0928 has a 2–10 keV rest-frame X-ray luminosity of $L_{2-10} = 11.6^{+4.3}_{-3.5} \times 10^{44}$ erg s^{-1}. Its X-ray-to-optical power-law slope is $\alpha_{\rm OX} = -1.67^{+0.16}_{-0.10}$, consistent with the general trend indicating that the X-ray emission in the most bolometrically powerful quasars is weaker relative to their optical emission.

Key words: cosmology: observations – early universe – quasars: individual (ULAS J134208.10+092838.61)

1. Introduction

Supermassive black holes are thought to be ubiquitous in the centers of massive galaxies, but their formation mechanism is still an outstanding question in astrophysics. The existence of distant quasars powered by $\gtrsim 10^9\,M_\odot$ black holes within the first Gyr of the universe sets one of the strongest challenges for supermassive black hole formation theories (e.g., Volonteri 2012). X-ray observations provide a unique tool to explore the immediate vicinities of the central black holes in active galactic nuclei (AGNs; e.g., Fabian 2016). Studying the evolution of X-ray properties and trends with luminosity across cosmic time teaches us about the physics of the inner regions of AGNs, potentially providing clues about the formation of supermassive black holes.

More than 200 quasars are now known within the first Gyr of the universe (i.e., at $z > 5.5$; e.g., Bañados et al. 2016; Wang et al. 2016), but only about a dozen of them have been robustly detected in X-rays (i.e., $\gtrsim$5 photons), only one of which is at $z > 6.5$ (Moretti et al. 2014; Page et al. 2014). Pioneering X-ray studies of the $z \sim 6$ quasar population based on 5–15 ks *Chandra* observations showed that their average X-ray properties are similar to those of low-redshift luminous quasars (Brandt et al. 2002; Shemmer et al. 2006). Recent deeper ($\gtrsim$50 ks) *Chandra* and *XMM-Newton* observations of a few $z > 6$ quasars have permitted meaningful constraints on key parameters of individual sources such as their photon index (Γ; e.g., Ai et al. 2017; Gallerani et al. 2017; Nanni et al. 2018), which is a tracer of the black hole accretion rate (e.g., Brightman et al. 2013).

Here, we report *Chandra* observations of the recently discovered redshift-record quasar ULAS J134208.10+092838.61 (hereafter J1342+0928) at $z = 7.54$ (Bañados et al. 2018). This quasar has a $7.8^{+3.3}_{-1.9} \times 10^8\,M_\odot$ accreting black hole and resides in a massive galaxy that is intensively forming stars (85–545 $M_\odot$ yr^{-1}; Venemans et al. 2017). Based on a 2.6 σ detection at 41 GHz, Venemans et al. (2017) classify this quasar as being potentially radio-loud with $R = S_{5,\rm GHz,rest}/S_{4400,\text{Å},\rm rest} = 12.4$ (see the discussion in their Section 3.2). Deeper radio observations are already accepted to confirm this preliminary result.

To directly compare with results from the literature (e.g., Nanni et al. 2017), we use a flat cosmology with $H_0 = 70$ km s^{-1} Mpc^{-1}, $\Omega_M = 0.3$, and $\Omega_\Lambda = 0.7$. We assume a Galactic absorption column density toward J1342+0928 of $N_{\rm H} = 1.61 \times 10^{20}$ cm^{-2} (Kalberla et al. 2005). Errors are reported at the 1σ (68%) confidence level unless otherwise stated. Upper limits correspond to 3σ limits.

2. Observations and Data Reduction

We observed J1342+0928 with *Chandra* for a total of 45.1 ks on 2017 December 15 (24.7 ks, Obs ID: 20124) and 2017 December 17 (20.4 ks, Obs ID: 20887). The detection image is shown in Figure 1. Observations were conducted with the Advanced CCD Imaging Spectrometer (ACIS; Garmire et al. 2003) using the Very Faint telemetry format and the Timed Exposure mode. *Chandra* was pointed so that J1342+0928 fell on the ACIS-S3 chip. We analyzed these data using `CIAO` version 4.9 (Fruscione et al. 2006) and CALDB version 4.7.7. Observations were combined using the `MERGE_OBS` routine to create images in the broad (0.5–7.0 keV) energy band. We used the ACIS standard filters for event grades (0, 2, 3, 4, and 6) and good time intervals.

We performed a source detection using `WAVDETECT` (Freeman et al. 2002), using scales of 1, 2, 4, 8, and 16 pixels and a point-spread function (PSF) map made from the weighted means of the two observations. A source was detected within $0\farcs19$ of J1342+0928, with $14.0^{+4.8}_{-3.7}$ net counts and a detection significance (net counts divided by background error) of 6σ. Due to the low number of counts in this source, we use the

[7] Carnegie-Princeton Fellow.

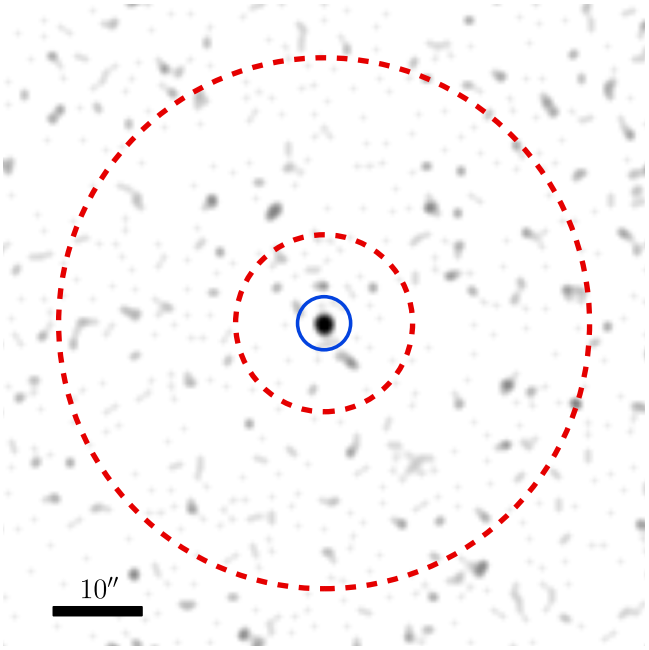

Figure 1. *Chandra* observation of J1342+0928. This image covers the energy range of 0.5–7.0 keV, was binned to pixels of size 0.″49, and has been smoothed with a Gaussian kernel of width 1.5 pixels (∼0.″75). The spectral extraction regions for the source (blue circle) and background (red annulus) are shown. We detect an X-ray source at the 6σ level within 1 pixel of the position reported by Bañados et al. (2018).

Gehrels (1986) approximation for uncertainties. `WAVDETECT` reported a PSFRATIO of 0.36 for this object, meaning that we do not find extended structure around this source and thus no evidence of powerful X-ray jets at our sensitivity (see also Fabian et al. 2014). No other sources were detected within 1.′0 of J1342+0928.

To characterize this source, we used `dmextract` to extract the total counts from 0.5–7.0 keV in a 3.″0 radius source aperture and a 10.″0 to 30.″0 background annulus. We detect $13.7^{+5.1}_{-4.0}$ net counts (in agreement with the `WAVDETECT` measurement), with an expected background of 2.3 counts. Following the binomial analysis technique used by Lansbury et al. (2014), we compute a probability of the X-ray detection of J1342+0928 being a false positive: $P = 4.3 \times 10^{-9}$ (5.8σ detection). Using the Bayesian techniques described by Park et al. (2006), assuming uniform (Jeffreys) priors[8] and integrating the joint posterior distribution with Gaussian quadrature in 1,000 bins, we compute an X-ray hardness ratio[9] of $\mathcal{HR} = -0.51^{+0.26}_{-0.28}$ across the 0.5–2.0 keV and 2.0–7.0 keV bands.

We extracted spectra in a 3.″0 radius aperture and a 10.″0 to 30.″0 background annulus from both observations around J1342+0928. Spectra were extracted in the energy range of 0.5–7.0 keV (4.3–59.8 keV in the rest frame of the quasar). Due to slight variations between the two pointings, an accurate response file cannot be generated from the combined image, so we instead extracted spectra from the two observations and combined them with the `CIAO` task `COMBINE_SPECTRA`. Fitting was performed with `PyXspec`, using `XSPEC` version 12.9.1 (Arnaud 1996).

We modeled the quasar spectrum with a combined power-law model (powerlaw) with Galactic absorption (phabs), using the modified c-statistic (Cash 1979; Wachter et al. 1979) to find best-fits and uncertainties. The source redshift was frozen to $z = 7.5413$ (Venemans et al. 2017) and the Galactic column density to $N_{\rm H} = 1.61 \times 10^{20}$ cm^{-2} (Kalberla et al. 2005). When allowed to vary, we found a best-fit value of $\Gamma = 1.95^{+0.55}_{-0.53}$. In a similar situation, Ai et al. (2016) reported a slope of $\Gamma = 3.0^{+0.8}_{-0.7}$ with a 14-count *Chandra* spectrum of a quasar at redshift $z = 6.33$. However, this value was then updated by Ai et al. (2017) to $\Gamma = 2.3 \pm 0.1$ using a deeper *XMM-Newton* spectrum with ∼460 counts. Due to the low number of source counts in our *Chandra* observation, we therefore base our fiducial values on a fit where we froze the power-law photon index to $\Gamma = 1.9$; this is a choice is based on the mean power-law index found for 10 $z \sim 6$ quasars studied by Nanni et al. (2017). The only free parameter was therefore the normalization of the power law. While Venemans et al. (2017) report a dust-rich host galaxy, its absorption effect is minor given the high energies at the redshift of the quasar we are probing with the *Chandra* observation. Even if we assume an absorber at the redshift of the X-ray source with column density $N_{\rm H} = 10^{23.5}$ cm^{-2}, the change in our measured luminosity compared to the fiducial value is less than the uncertainties in the original measurement. As higher levels of obscuration for sources with comparable X-ray luminosity is only expected in dust-obscured galaxies (DOGS) and hot DOGS (Vito et al. 2018), we cannot place any significant constraints on this absorption without deeper observations.

Assuming a power-law index of $\Gamma = 1.9$, we find that the absorption-corrected flux of J1342+0928 from 0.5–2.0 keV (observed) is $F_{0.5-2.0} = 1.68^{+0.52}_{-0.44} \times 10^{-15}$ erg s^{-1} cm^{-2} and the luminosity at rest-frame 2–10 keV is $L_{2-10} = 11.6^{+4.3}_{-3.5} \times 10^{44}$ erg s^{-1}. As the spectral response of our *Chandra* observations did not cover the full 2–10 keV rest-frame energy band, the measured luminosity is extrapolated using the best-fit model. To account for the uncertainty in the value of Γ, we also find the flux and luminosities for models with $\Gamma = 1.6$ and $\Gamma = 2.2$. We find for $\Gamma = 1.6$, $F_{0.5-2.0} = 1.44^{+0.45}_{-0.37} \times 10^{-15}$ erg s^{-1} cm^{-2} and $L_{2-10} = 8.9^{+3.3}_{-2.7} \times 10^{44}$ erg s^{-1}, while for $\Gamma = 2.2$, $F_{0.5-2.0} = 1.94^{+0.60}_{-0.50} \times 10^{-15}$ erg s^{-1} cm^{-2} and $L_{2-10} = 15.3^{+5.7}_{-4.6} \times 10^{44}$ erg s^{-1}. When using the free-to-vary value of Γ ($\Gamma = 1.95$), we measure $F_{0.5-2.0} = 1.71^{+0.54}_{-0.45} \times 10^{-15}$ erg s^{-1} cm^{-2} and $L_{2-10} = 13.0^{+4.0}_{-3.4} \times 10^{44}$ erg s^{-1}.

3. Discussion

The X-ray detection of J1342+0928 at $z = 7.54$ is robust (see Figure 1), but deeper *Chandra* or *XMM-Newton* observations will be crucial in order to derive meaningful X-ray spectral parameters. J1342+0928 represents the most distant non-transient astronomical source identified in X-rays to date[10] and its $L_{2-10} = 11.6^{+4.3}_{-3.5} \times 10^{44}$ erg s^{-1} luminosity is consistent with the luminosities observed in other $z > 5.6$ quasars (see Figure 2).

The properties of the most distant quasars are so extreme that it is often challenging to find lower-redshift quasars with analogous properties (see, e.g., discussion in Bañados et al.

[8] Assuming flat priors on θ only changed our reported value of $\mathcal{HR}$ by $\sim 0.25\sigma$.

[9] $\mathcal{HR} = (H - S)/(H + S)$, where H and S are the net counts in the hard (2.0–7.0 keV) and soft (0.5–2.0 keV) bands, respectively.

[10] We note that gamma-ray bursts have been detected in X-rays up to $z = 8.23 + 0.07 - 0.08$ (Tanvir et al. 2009). See Salvaterra (2015) for a summary of the highest-redshift gamma-ray bursts.

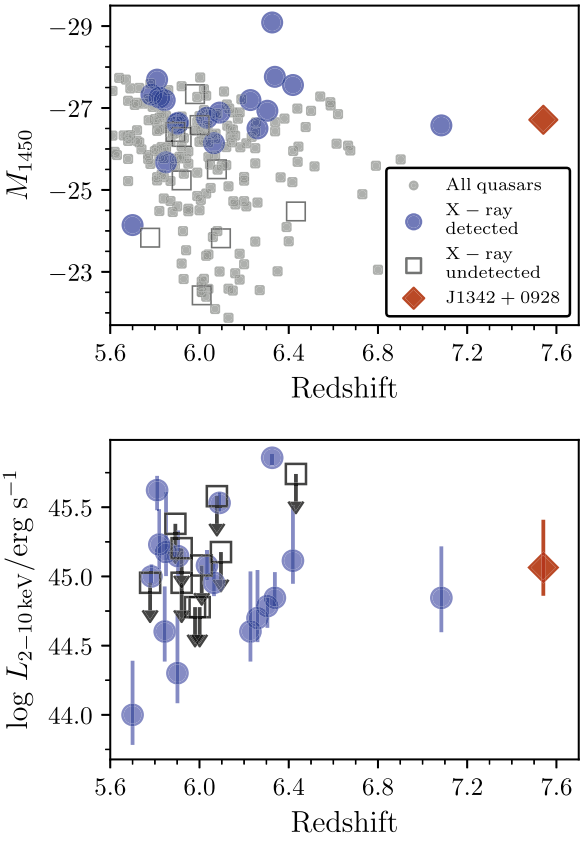

Figure 2. Top: absolute magnitude at rest-frame wavelength 1450 Å for all $z > 5.6$ quasars known to date. High-redshift quasars with X-ray observations (as compiled by Nanni et al. 2017, 2018) are represented by filled blue circles for detections and open squares for non-detections. The quasar studied in this work, J1342+0928, is shown as a red diamond. Bottom: rest-frame 2–10 keV luminosity for $z > 5.6$ quasars with X-ray observations (all X-ray luminosities are taken from Nanni et al. 2017, except for J1342+0928 (this work) and J1030 +0524 at $z = 6.31$, which is taken from Nanni et al. 2018, who reported an updated value of the rest-frame 2–8 keV luminosity). Symbols follow the same legend as the top panel. The uncertainties in the X-ray luminosity for J1342 +0928 correspond to the values allowed by assuming a photon index $\Gamma = 1.6$ and $\Gamma = 2.2$, while the data point is shown assuming our fiducial value of $\Gamma = 1.9$. Upper limits are reported at the 3σ level.

2018; Davies et al. 2018). Recently, in a series of papers, Bischetti et al. (2017), Duras et al. (2017), Martocchia et al. (2017), and Vietri et al. (2018) reported the physical properties of the $z \sim 2$–4 *WISE*/SDSS selected hyperluminous (WISSH) quasar sample. The WISSH quasars have bolometric luminosities $L_{\mathrm{Bol}} \gtrsim 10^{47}$ erg s^{-1}, $\gtrsim 10^{9}\,M_{\odot}$ black holes accreting near the Eddington limit, host galaxies with star formation rates up to $\sim 2000\,M_{\odot}$ yr^{-1}, and show signatures of powerful ionized outflows manifested as broad [O III] emission lines and C IV blueshifts greater than 2000 km s^{-1}. These characteristics are similar and in some cases even more extreme than the properties of the most distant quasars known to date (cf. Leipski et al. 2014; Mazzucchelli et al. 2017).

Martocchia et al. (2017) reported that the WISSH quasars show a low X-ray-to-optical flux ratio compared with other lower-redshift AGNs/quasars with similar X-ray luminosities (see their Figure 4). A similar trend had already been reported for some of the most optically hyperluminous ($M_i < -29$) SDSS quasars studied by Just et al. (2007) at $z \sim 1.5$–4.5. Other extreme sources such as the hyperluminous $z \sim 2$ hot DOGS studied by Vito et al. (2018) also show hints of weaker X-ray emission than expected from their large mid-infrared luminosities. These studies are suggesting that the X-ray flux saturates for more bolometrically powerful quasars, while the ultraviolet and mid-infrared luminosities still increase (e.g., Stern 2015; Chen et al. 2017), although larger samples of the most luminous objects are still required to robustly confirm this picture. The lamppost model of the X-ray corona (e.g., Miniutti & Fabian 2004) provides a plausible physical scenario to explain this observation. In this model, the X-ray corona is a compact plasma along the black hole spin axis, potentially associated with the base of the jet. The hot corona Compton upscatters photons from the accretion disk to higher energies, creating much of the high-energy emission observed from AGNs. In this lamppost model, more luminous systems might push the corona to greater heights, thereby lowering its geometrical cross section with the seed accretion disk photons, and causing the observed sublinear relation between X-ray emission and both ultraviolet and mid-infrared emission.

Interestingly, intrinsically weak X-ray emission has also been interpreted as a requirement to explain powerful quasar outflows in order to avoid the suppression of ultraviolet line driven winds (Richards et al. 2011; Luo et al. 2013, 2015). Mazzucchelli et al. (2017) recently showed that large C IV blueshifts are common in quasars at $z > 6.5$ (with a median of $\sim$2400 km s^{-1}). J1342+0928 is one of the most extreme examples among these objects, presenting a C IV emission line blueshifted by $\sim$6100 km s^{-1} from the Mg II line and $\sim$6600 km s^{-1} from the systemic redshift based on the [C II] emission line (Bañados et al. 2018). This gives us the opportunity to test whether these powerful quasars with strong outflows at very different redshifts have common X-ray properties.

The X-ray-to-optical flux ratio ($L_{2-10}/L_{2500\text{Å}}$) for J1342 +0928 is 0.04, which is similar to the values reported for the WISSH sample (see Figure 4 in Martocchia et al. 2017). A more common term used in the literature is the X-ray-to-optical power-law slope defined as the index of the power law connecting the monochromatic luminosities at 2 kev and 2500 Å: $\alpha_{\mathrm{OX}} = 0.3838 \times \log(L_{2\mathrm{keV}}/L_{2500\text{Å}})$. In Figure 3, we show α_{OX} as a function of the rest-frame 2500 Å monochromatic luminosity for all $z \gtrsim 6$ quasars compiled by Nanni et al. (2017, 2018), J1342+0928 (this work), and the Just et al. and Martocchia et al. quasar samples. With $\alpha_{\mathrm{OX}} = -1.67^{+0.16}_{-0.10}$ and $L_{2500\text{Å}} = 10^{31.42}$ erg s^{-1} Hz^{-1}, measured directly from its spectrum, J1342+0928 falls right on the relations found by Martocchia et al. (2017) and Nanni et al. (2017) (see Figure 3). We note that the reported α_{OX} assumes that the quasar luminosity did not vary between the near-infrared and X-ray observations, which were taken about nine months apart. Almost all of the most distant quasars occupy a locus in Figure 3 that bridges the typical AGN (Lusso & Risaliti 2016) and the extreme WISSH quasars and the hyperluminous quasars from Just et al. (2007). The lone exception is RD J1148+5253 at $z = 5.7$ (Mahabal et al. 2005), which is one of the optically faintest quasars known at $z > 5.5$. The properties of RD J1148+5253 are more similar to the quasars from thee Palomar-Green (PG) bright quasar survey (Laor et al. 1994). The WISSH and the hyperluminous SDSS quasars therefore seem to share similar X-ray and optical properties with the most distant quasars. A detailed comparison between these two samples could shed light into the understanding of some of the most extreme sources known in the universe.

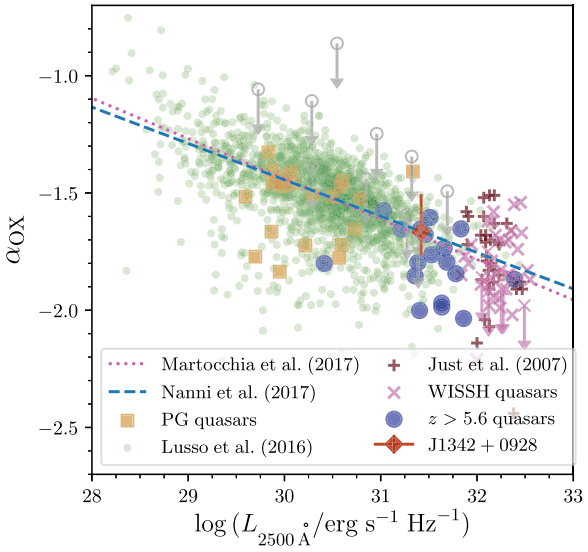

Figure 3. X-ray-to-optical power-law slope (α_{OX}) as a function of the rest-frame 2500 Å monochromatic luminosity. The green small circles represent the AGNs from Lusso & Risaliti (2016) with X-ray detections with a signal-to-noise ratio greater than five. We also show the quasars from the Palomar-Green (PG) bright quasar survey (Laor et al. 1994), the hyperluminous SDSS quasars studied by Just et al. (2007), and the *WISE*/SDSS selected hyperluminous (WISSH) quasar sample (Martocchia et al. 2017) as orange rectangles, maroon plusses, and pink crosses, respectively. The $z > 5.6$ quasars (circles) and J1342 +0928 (red diamond; this work) occupy the locus in between the Lusso & Risaliti (2016) AGNs and the quasar samples of Just et al. (2007) and Martocchia et al. (2017). In the calculation of α_{OX} for the $z > 5.6$ quasars we used the X-ray fluxes reported by Nanni et al. (2017, 2018) and the rest-frame 2500 Å flux densities, extrapolating the 1450 Å rest-frame magnitudes (see Figure 2), assuming a typical ultraviolet–optical power-law slope of $\alpha_\nu = -0.5$ (e.g., Bañados et al. 2015). The dotted and dashed lines are the best-fit relation between α_{OX} and $L_{2500\text{Å}}$ reported by Martocchia et al. (2017) and Nanni et al. (2017), respectively. The uncertainty in α_{OX} for J1342+0928 is dominated by the systematic uncertainty in the X-ray luminosity as it was calculated fixing the power-law photon index to $\Gamma = 1.9$ (see the text).

Recently, Risaliti & Lusso (2015) and Lusso & Risaliti (2017) have proposed that under some assumptions quasars can be used as standard candles. This is based on the tight relation between the X-ray and ultraviolet emission (see Figure 3) coupled with the full-width at half maximum (FWHM) of the Mg II line. At face value, J1342+0928 follows the relation ($L_{2\text{keV}} \propto L_{2500\text{Å}}^{4/7}\, v_{\text{fwhm}}^{4/7}$) reported in Figure 2 of Lusso & Risaliti (2017) within the uncertainties. Although this will need to be confirmed with deeper data and more $z > 7$ quasars, the present X-ray detection of an accreting black hole at $z = 7.54$ opens up the exciting prospect of testing the cosmological model when the universe was only 5% of its current age.

We thank the referee for useful comments that improved this Letter. We thank Silvia Martocchia for providing the data to produce Figure 3. The work of D.S. was carried out at the Jet Propulsion Laboratory, California Institute of Technology, under a contract with NASA. B.P.V. and F. Walter acknowledge funding through ERC grants "Cosmic Dawn" and "Cosmic Gas." The scientific results reported in this article are based on observations made by the *Chandra* X-ray Observatory. This research has made use of software provided by the *Chandra* X-ray Center (CXC) in the application package CIAO.

Facility: CXO.

Software: Astropy (Astropy Collaboration et al. 2018).

ORCID iDs

Eduardo Bañados https://orcid.org/0000-0002-2931-7824
Thomas Connor https://orcid.org/0000-0002-7898-7664
Daniel Stern https://orcid.org/0000-0003-2686-9241
Xiaohui Fan https://orcid.org/0000-0003-3310-0131
Roberto Decarli https://orcid.org/0000-0002-2662-8803
Emanuele P. Farina https://orcid.org/0000-0002-6822-2254
Chiara Mazzucchelli https://orcid.org/0000-0002-5941-5214
Bram P. Venemans https://orcid.org/0000-0001-9024-8322
Fabian Walter https://orcid.org/0000-0003-4793-7880
Feige Wang https://orcid.org/0000-0002-7633-431X
Jinyi Yang https://orcid.org/0000-0001-5287-4242

References

Ai, Y., Dou, L., Fan, X., et al. 2016, ApJL, 823, L37
Ai, Y., Fabian, A. C., Fan, X., et al. 2017, MNRAS, 470, 1587
Arnaud, K. A. 1996, in ASP Conf. Ser. 101, Astronomical Data Analysis Software and Systems V, ed. G. H. Jacoby & J. Barnes (San Francisco, CA: ASP), 17
Astropy Collaboration, Price-Whelan, A. M., Sipőcz, B. M., et al. 2018, arXiv:1801.02634
Bañados, E., Venemans, B. P., Decarli, R., et al. 2016, ApJS, 227, 11
Bañados, E., Venemans, B. P., Mazzucchelli, C., et al. 2018, Natur, 553, 473
Bañados, E., Venemans, B. P., Morganson, E., et al. 2015, ApJ, 804, 118
Bischetti, M., Piconcelli, E., Vietri, G., et al. 2017, A&A, 598, A122
Brandt, W. N., Schneider, D. P., Fan, X., et al. 2002, ApJL, 569, L5
Brightman, M., Silverman, J. D., Mainieri, V., et al. 2013, MNRAS, 433, 2485
Cash, W. 1979, ApJ, 228, 939
Chen, C.-T. J., Hickox, R. C., Goulding, A. D., et al. 2017, ApJ, 837, 145
Davies, F. B., Hennawi, J. F., Bañados, E., et al. 2018, arXiv:1801.07679
Duras, F., Bongiorno, A., Piconcelli, E., et al. 2017, A&A, 604, A67
Fabian, A. C. 2016, AN, 337, 375
Fabian, A. C., Walker, S. A., Celotti, A., et al. 2014, MNRAS, 442, L81
Freeman, P. E., Kashyap, V., Rosner, R., & Lamb, D. Q. 2002, ApJS, 138, 185
Fruscione, A., McDowell, J. C., Allen, G. E., et al. 2006, Proc. SPIE, 6270, 62701V
Gallerani, S., Zappacosta, L., Orofino, M. C., et al. 2017, MNRAS, 467, 3590
Garmire, G. P., Bautz, M. W., Ford, P. G., Nousek, J. A., & Ricker, G. R., Jr. 2003, Proc. SPIE, 4851, 28
Gehrels, N. 1986, ApJ, 303, 336
Just, D. W., Brandt, W. N., Shemmer, O., et al. 2007, ApJ, 665, 1004
Kalberla, P. M. W., Burton, W. B., Hartmann, D., et al. 2005, A&A, 440, 775
Lansbury, G. B., Alexander, D. M., Del Moro, A., et al. 2014, ApJ, 785, 17
Laor, A., Fiore, F., Elvis, M., Wilkes, B. J., & McDowell, J. C. 1994, ApJ, 435, 611
Leipski, C., Meisenheimer, K., Walter, F., et al. 2014, ApJ, 785, 154
Luo, B., Brandt, W. N., Alexander, D. M., et al. 2013, ApJ, 772, 153
Luo, B., Brandt, W. N., Hall, P. B., et al. 2015, ApJ, 805, 122
Lusso, E., & Risaliti, G. 2016, ApJ, 819, 154
Lusso, E., & Risaliti, G. 2017, A&A, 602, A79
Mahabal, A., Stern, D., Bogosavljević, M., Djorgovski, S. G., & Thompson, D. 2005, ApJL, 634, L9
Martocchia, S., Piconcelli, E., Zappacosta, L., et al. 2017, A&A, 608, A51
Mazzucchelli, C., Bañados, E., Venemans, B. P., et al. 2017, ApJ, 849, 91
Miniutti, G., & Fabian, A. C. 2004, MNRAS, 349, 1435
Moretti, A., Ballo, L., Braito, V., et al. 2014, A&A, 563, A46
Nanni, R., Gilli, R., Vignali, C., et al. 2018, arXiv:1802.05613
Nanni, R., Vignali, C., Gilli, R., Moretti, A., & Brandt, W. N. 2017, A&A, 603, A128
Page, M. J., Simpson, C., Mortlock, D. J., et al. 2014, MNRAS, 440, L91
Park, T., Kashyap, V. L., Siemiginowska, A., et al. 2006, ApJ, 652, 610
Richards, G. T., Kruczek, N. E., Gallagher, S. C., et al. 2011, AJ, 141, 167
Risaliti, G., & Lusso, E. 2015, ApJ, 815, 33
Salvaterra, R. 2015, JHEAp, 7, 35
Shemmer, O., Brandt, W. N., Schneider, D. P., et al. 2006, ApJ, 644, 86
Stern, D. 2015, ApJ, 807, 129
Tanvir, N. R., Fox, D. B., Levan, A. J., et al. 2009, Natur, 461, 1254
Venemans, B. P., Walter, F., Decarli, R., et al. 2017, ApJL, 851, L8
Vietri, G., Piconcelli, E., Bischetti, M., et al. 2018, arXiv:1802.03423
Vito, F., Brandt, W. N., Stern, D., et al. 2018, MNRAS, 474, 4528
Volonteri, M. 2012, Sci, 337, 544
Wachter, K., Leach, R., & Kellogg, E. 1979, ApJ, 230, 274
Wang, F., Wu, X.-B., Fan, X., et al. 2016, ApJ, 819, 24